Directional Interactions between Membrane Proteins

Christoph A. Haselwandter[1,2] and Rob Phillips[2]

[1]*Department of Physics and Astronomy, University of Southern California, Los Angeles, California 90089, USA*
[2]*Department of Applied Physics, California Institute of Technology, Pasadena, California 91125, USA*
(Dated: September 17, 2012)

While modern structural biology has provided us with a rich and diverse picture of membrane proteins, the biological function of membrane proteins is often influenced by the mechanical properties of the surrounding lipid bilayer. Here we develop an analytic methodology connecting the hydrophobic shape of membrane proteins to the cooperative function of membrane proteins induced by bilayer-mediated elastic interactions. Application of this methodology to mechanosensitive channels shows that, in addition to protein separation and bilayer material properties, the sign and strength of elastic interactions, and associated cooperative gating characteristics, can depend on the protein shape and orientation. Our approach predicts how elastic interactions affect the molecular structure, organization, and biological function of proteins in crowded membranes.

Cell membranes exhibit a complex organization of lipids and membrane proteins [1, 2] and play an integral role in many cellular processes. The functional properties of membrane proteins are not purely determined by protein structure but, rather, membrane proteins act in concert with the surrounding lipid bilayer [3–7]. In particular, the hydrophobic regions of membrane proteins couple to the hydrophobic regions of lipid bilayers [8–11]. The energetic cost of the resulting membrane deformations can be captured by an elastic model [12–18] in which the lipid bilayer is described as an elastic medium and the membrane proteins are regarded as rigid membrane inclusions. Neighboring membrane proteins may induce overlapping deformation fields of the bilayer membrane, yielding long-range interactions between membrane proteins [16, 19]. Experiments have implicated such membrane-mediated interactions in the clustering of a number of different membrane proteins [19–25].

Theoretical studies of membrane-mediated interactions between proteins [16, 26–37] have mainly focused on the idealized case of cylindrical or conical membrane inclusions at large separations. However, cell membranes are crowded [38–40], with the size and spacing of membrane proteins both being of the order of a few nanometers. In addition, structural studies [41, 42] have shown that membrane proteins exhibit a rich variety of hydrophobic shapes. How are the shapes of neighboring membrane proteins reflected in the structure of elastic bilayer deformations, and what are the resulting directional interactions between membrane proteins at the small separations most relevant for cell membranes? In this Letter we describe an analytic methodology for estimating directional interactions between membrane proteins for arbitrary protein separations. We first develop our general methodology, and then apply this methodology to the mechanosensitive channel of large conductance (MscL) [43–47]. Our calculation of the interaction potentials and cooperative gating curves for the proposed pentameric

structures of MscL [41, 47–57] shows that, similarly as lipid bilayer material properties [12–18, 25, 54–57], elastic interactions can alter the structure and function of proteins in crowded membranes.

Following the standard framework of membrane elasticity [58–60], we describe the positions of the inner and outer lipid bilayer leaflets within the Monge representation through the functions $h_+(x,y)$ and $h_-(x,y)$, which determine [61] the midplane and thickness deformation fields governing bilayer membranes. Since thickness deformations are thought to be dominant for MscL gating [62–65], we illustrate our methodology for the thickness deformation field $u(x,y) = \frac{1}{2}\left[h_+(x,y) - h_-(x,y) - 2a\right]$, where $2a$ is the hydrophobic thickness of the unperturbed lipid bilayer, with the elastic energy [12, 26, 58–67]

$$G = \tfrac{1}{2} \int dx\,dy \left\{ K_b(\nabla^2 u)^2 + K_t\left(\tfrac{u}{a}\right)^2 + \tau\left[2\tfrac{u}{a} + (\nabla u)^2\right] \right\},$$

(1)

where K_b is the bending rigidity of the lipid bilayer, K_t is the stiffness associated with thickness deformations, and τ is the membrane tension. Midplane deformations decouple to leading order from thickness deformations [61], and are described [58–65] by an energy functional similar to Eq. (1). For generality we allow for the two tension terms u/a and $(\nabla u)^2$ in Eq. (1), which capture the effects of membrane tension on lipid surface area [60, 64, 65] and on membrane undulations [58–63], respectively.

The Euler-Lagrange equation associated with Eq. (1) is given by

$$\left(\nabla^2 - \nu_+\right)\left(\nabla^2 - \nu_-\right)\bar{u} = 0\,,$$

(2)

where $2K_b\nu_\pm = \tau \pm \left(\tau^2 - 4K_bK_t/a^2\right)^{1/2}$ and $\bar{u} = u + \tau a/K_t$. The solution of Eq. (2) for a single cylindrical membrane inclusion of radius R_i is [12, 68]

$$\bar{u}(r_i,\theta_i) = f_i^+(r_i,\theta_i) + f_i^-(r_i,\theta_i)\,,$$

(3)

where r_i and θ_i are polar coordinates with the center of inclusion i as the origin, the Fourier-Bessel se-

ries $f_i^{\pm}(r_i, \theta_i) = A_{i,0}^{\pm} K_0(\sqrt{\nu_{\pm}} r_i) + \sum_{n=1}^{\infty} (\mathcal{A}_{i,n} + \mathcal{B}_{i,n})$, in which $\mathcal{A}_{i,n} = A_{i,n}^{\pm} K_n(\sqrt{\nu_{\pm}} r_i) \cos n\theta_i$ and $\mathcal{B}_{i,n} = B_{i,n}^{\pm} K_n(\sqrt{\nu_{\pm}} r_i) \sin n\theta_i$, K_n are modified Bessel functions of the second kind, and we have assumed that membrane deformations decay away from a single membrane inclusion [66]. The coefficients $A_{i,n}^{\pm}$ and $B_{i,n}^{\pm}$ are determined by the boundary conditions at the bilayer-inclusion interface for which, consistent with previous studies [12, 26, 62–67], we use

$$u(r_i, \theta_i)\big|_{r_i=R_i} = U_i(\theta_i), \qquad (4)$$

$$\hat{\mathbf{n}} \cdot \nabla u(r_i, \theta_i)\big|_{r_i=R_i} = U_i'(\theta_i), \qquad (5)$$

where $\hat{\mathbf{n}}$ is the unit normal vector along the bilayer-inclusion interface.

Following Refs. [27, 31] we construct the solution of Eq. (2) appropriate for two cylindrical membrane inclusions of radius R_1 and R_2 using the ansatz

$$u = u_1(r_1, \theta_1) + u_2(r_2, \theta_2), \qquad (6)$$

where the $u_i(r_i, \theta_i)$ are the single-inclusion deformation fields implied by Eq. (3), with the bipolar coordinate transformations $r_2 = \left(d^2 + r_1^2 + 2dr_1 \cos\theta_1\right)^{1/2}$, $\cos\theta_2 = (d + r_1 \cos\theta_1)/r_2$, and $\sin\theta_2 = (r_1 \sin\theta_1)/r_2$, in which d is the center-to-center distance between the two inclusions. Note that, if the single-inclusion solution in Eq. (3) is considered up to some order $n = N$, Eq. (6) contains $4(2N + 1)$ independent constants which must be fixed through the boundary conditions in Eqs. (4) and (5). Employing Eq. (2), the elastic energy in Eq. (1) can then be written as a sum over the boundary terms

$$G_i = -\frac{R_i}{2} \int_0^{2\pi} d\theta_i \left(K_b \frac{\partial \bar{u}}{\partial r_i} \nabla^2 \bar{u} - K_b \bar{u} \frac{\partial}{\partial r_i} \nabla^2 \bar{u} + \tau \bar{u} \frac{\partial \bar{u}}{\partial r_i} \right) \qquad (7)$$

at $r_i = R_i$, where we have neglected terms independent of $\bar{u}$. This expression is evaluated at each order in the Fourier-Bessel series in Eq. (6) using the orthogonality properties of trigonometric functions. Thus, the elastic energy in Eq. (1) reduces to an algebraic expression for the coefficients $A_{i,n}^{\pm}$ and $B_{i,n}^{\pm}$ which, in turn, are prescribed by the boundary conditions in Eqs. (4) and (5).

We determine the coefficients $A_{i,n}^{\pm}$ and $B_{i,n}^{\pm}$ in Eq. (6) up to arbitrary N by expanding u_2 in the membrane region surrounding inclusion 1 in terms of r_1/d and imposing on u the boundary conditions at $r_1 = R_1$ [27, 31], with a similar procedure for inclusion 2. Thus, finding the general solution in Eq. (6) which respects the boundary conditions in Eqs. (4) and (5) reduces to solving a system of $4(2N+1)$ linear equations, which we achieve using standard methods [69]. Substitution of the resulting expressions of the coefficients into Eq. (7) yields, for a given N, the interaction potential between two membrane inclusions. The validity of this finite-order series solution is based on the assumption that very rapid angular variations at large n in the membrane deformation field can be

neglected, which we confirm for a given problem by systematically including higher-order terms. We have verified [70] this methodology for the analytic calculation of elastic interaction potentials in the case of cylindrical membrane inclusions of constant hydrophobic thickness, for which elastic interaction potentials were calculated previously [24, 64] using computer simulations.

We now apply the above methodology to estimate elastic interactions between MscL proteins. In the most basic scenario, MscL can exist in one of two states—open or closed—with the competition between these two states governed by membrane tension [43–47]. A simple coarse-grained model of the cross-sectional shape of MscL is

$$C_i(\theta_i) = R_i \left[1 + \epsilon_i \cos s \left(\theta_i - \omega_i\right)\right], \qquad (8)$$

where ϵ_i parameterizes the magnitude of the deviation of the protein cross section from the circle, s denotes the order of the protein symmetry (oligomeric state), and ω_i captures the orientation of the protein [see insets in Fig. 1 for illustrations of Eq. (8)]. The physiologically relevant oligomeric states of MscL remain a matter of debate [47–50], with tetrameric [71], pentameric [51], and hexameric [72] MscL having been reported. Our methodology is able to handle all of these cases, but here we focus on pentameric MscL, which correspond to $s = 5$ in Eq. (8) with R_i and ϵ_i estimated from structural models [41, 51–57]. Since these structural models of MscL suggest $\epsilon_i \ll 1$, we concentrate on the weak perturbation limit of Eq. (8) and only consider the leading-order terms in ϵ_i breaking rotational symmetry. Expansion of u at $r_i = C_i(\theta_i)$ in ϵ_i [34, 36] yields boundary conditions of the form in Eqs. (4) and (5). For simplicity we first consider the case of a constant U_i along $C_i(\theta_i)$, with a value of a so that U_i is of the same sign in the open and closed states of MscL, and then turn to the complementary case of directional interactions induced by a varying U_i [10, 11]. We choose [70] the parameter values for bilayer-MscL interactions as discussed in Refs. [62–65] and, in particular, set $U_i'(\theta_i) = 0$ along the bilayer-MscL interface.

Figure 1(a) shows the elastic interaction potentials between pentameric MscL proteins in the open state [41, 52–55], with similar curves for the corresponding closed state structure [51]. Irrespective of the relative protein orientation considered, we find an energy barrier to the dimerization of two open (or closed) MscL proteins. For most protein separations, the tip-on orientation is energetically most favorable with the face-on orientation being least favorable. For very small d, however, the face-on orientation becomes favorable over the tip-on orientation [see inset in Fig. 1(a)]. Figure 1(b) demonstrates that elastic interactions between open and closed MscL proteins can also yield an energy barrier to dimerization. But, in contrast to Fig. 1(a), MscL proteins now repel each other at very small d, and we obtain a pronounced minimum in the interaction energy at some optimal value of d which depends on the relative protein
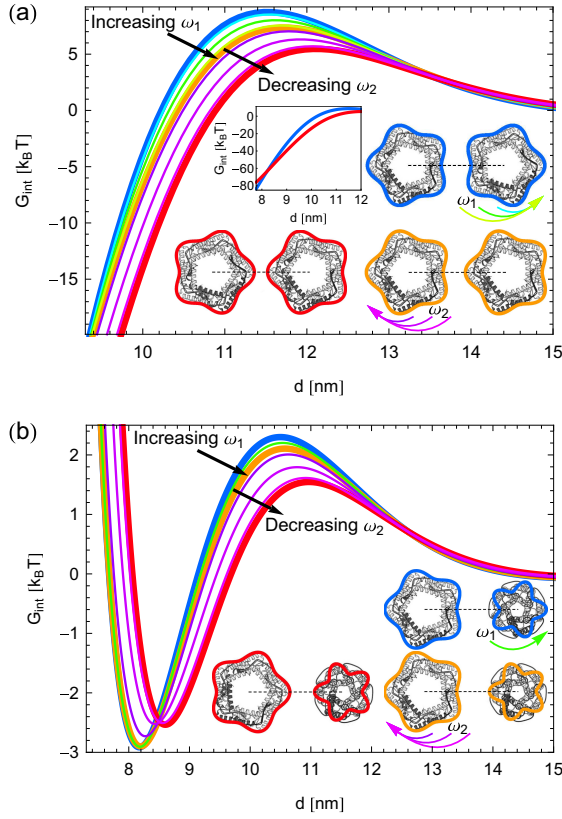
FIG. 1: (color online). Elastic interaction potentials obtained from Eq. (7) for (a) open and (b) open and closed MscL. Bilayer-MscL interactions were parameterized [70] as in Ref. [65] but for a PC20 lipid bilayer with $\tau = 0$. Thick curves denote the three MscL orientations in the insets, while thin curves correspond to intermediate MscL orientations rotated by $\pi/20$ or $\pi/10$ as indicated by arrows. The molecular models of MscL in the insets are taken from Ref. [41] and the superimposed boundary curves were obtained from Eq. (8) with $R_i \approx 3.49$ nm and $R_i \approx 2.27$ nm [70] for open and closed MscL.
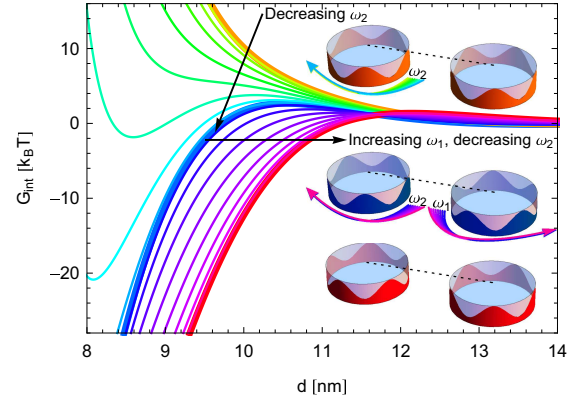

FIG. 2: (color online). Elastic interaction potentials obtained from Eq. (7) for cylindrical membrane inclusions of radius $R_i = 3.5$ nm with the hydrophobic mismatch in Eq. (9). The lipid bilayer was parameterized [70] as in Ref. [64] with $\tau = 0$. Thick curves denote the three inclusion orientations in the insets, while thin curves correspond to intermediate orientations rotated by $\pi/45$ as indicated by arrows.

orientation. Similarly as in the case of two open MscL proteins, the tip-on orientation is energetically most favorable, and the face-on orientation least favorable, for most protein separations in Fig. 1(b), with the tip-on orientation becoming least favorable for very small d. For all scenarios in Fig. 1 we find that G changes smoothly upon rotation from the face-on to the tip-on orientation.

The analytic solution in Eq. (6) in terms of single-inclusion deformation fields suggests a simple qualitative explanation for the non-monotonic behavior of the MscL interaction potentials in Fig. 1. In general, the single-inclusion thickness deformation field in Eq. (3) overshoots considerably [12, 26] at its first extremum when relaxing away from the inclusion boundary. Hence, if two channels induce thickness deformations of the same sign, there is a regime of intermediate d for which membrane deformations are amplified, yielding the energy barriers in Fig. 1. At small d, the membrane deformation fields

already overlap before reaching the first extremum, thus reducing the overall deformation footprint of the two channels and making dimerization favorable as implied by Fig. 1. For membrane channels of distinct hydrophobic thickness, however, moving the channels even closer together yields an additional regime in which the membrane has to deform strongly between the two channels, leading to repulsion between open and closed MscL at very small d as in Fig. 1(b). In each of these regimes, the competition between tip-on and face-on orientations is governed by a complex interplay between the local strengths and associated membrane areas of overlapping deformation fields.

The qualitative picture of elastic interaction potentials developed above for the boundary curves in Eq. (8) also applies to the complementary case of directional interactions induced by a varying hydrophobic thickness of membrane proteins [10, 11]. To illustrate this scenario we consider cylindrical membrane inclusions with hydrophobic mismatch

$$U_i(\theta_i) = U_i^0 + \delta_i \cos s \left(\theta_i - \omega_i \right) , \qquad (9)$$

where U_i^0 is the average hydrophobic mismatch and δ_i is the magnitude of mismatch modulations [see insets in Fig. 2 for illustrations of Eq. (9)]. Figure 2 shows the interaction potentials associated with Eq. (9). A striking feature of Fig. 2 is that, depending on the relative inclusion orientation, membrane-mediated interactions can be attractive or repulsive at small d. In particular, if the periodic modulations in Eq. (9) are in phase at the closest approach of the two inclusions there is, again due to the oscillatory nature of the single-inclusion deformation fields, an energy barrier to dimerization as in Fig. 1(a), with attraction at small d. Conversely, in the case of ori-
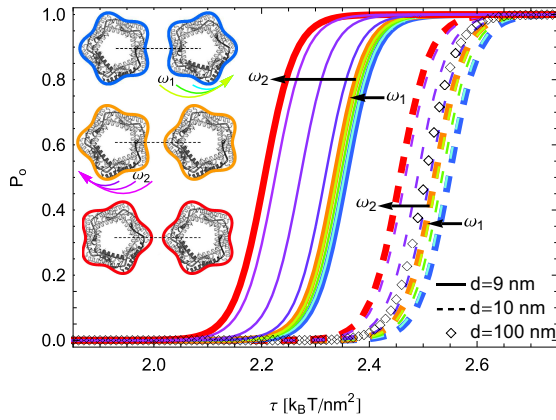
FIG. 3: (color online). Gating curves for a pair of MscL proteins to transition from the open-closed to the open-open configuration [see Figs. 1(b) and 1(a)] for the lipid bilayer parameter values [70] in Ref. [64]. The gating curves at $d = 9$ nm and $d = 10$ nm for different protein orientations are labelled as in Fig. 1(a). The molecular models in the insets are taken from Ref. [41], and we use the same boundary curves for open and closed states of MscL as in Fig. 1.

entations in Fig. 2 for which the periodic modulations in Eq. (9) are out of phase at the closest approach of the two inclusions, opposing inclusion boundaries induce distinct thickness deformations which, similarly as in Fig. 1(b), can lead to repulsion at small d. The interaction potentials in Fig. 2 change smoothly upon rotation from out-of-phase to in-phase orientations, and exhibit a minimum for intermediate orientations.

Interaction potentials such as those in Figs. 1 and 2 can induce directionality in the cooperative function of membrane proteins. In particular, the gating characteristics of MscL with varying membrane tension are captured [43–45] by the channel opening probability $P_o = 1/\left[1 + e^{\beta(\Delta G - \tau \Delta A)}\right]$, where $\beta = 1/k_B T$, in which k_B is Boltzmann's constant and T is the temperature, and ΔG and ΔA are the free energy and area difference between open and closed channel states. We only consider here contributions to ΔG due to thickness deformations of the bilayer membrane in Eq. (7), which were found previously [24, 62–65] to yield the basic phenomenology of MscL gating. Figure 3 shows P_o for pentameric MscL [41, 47–57] with a neighboring pentameric MscL protein in the open state. We find that, compared to the case of non-interacting MscL, membrane-mediated interactions can, depending on the protein separation and orientation, shift the gating tension to higher as well as lower values. The magnitude of the effect of directional interactions in Fig. 3 is comparable to previously measured [25, 54] shifts in gating tension due to modification of the membrane composition. As expected from the interaction potentials in Fig. 1, the cooperative gating tension associated with the tip-on orientation is lower than the cooperative gating tension associated with the face-on

orientation for the protein separations in Fig. 3, with a smooth interpolation in P_o between these two limiting orientations.

In summary, we have developed an analytic methodology for estimating directional interactions between membrane proteins for arbitrary protein separations. This methodology provides a bridge connecting the hydrophobic shape of membrane proteins to the cooperative function of membrane proteins induced by elastic interactions. Our methodology is general and can be applied to any membrane protein for which basic structural information is available. On the basis of a simple model of the cross-sectional shape of MscL suggested by structural studies [41, 47–57], we predict that bilayer-mediated interactions between MscL proteins yield a characteristic sequence of preferred orientations, and distinctive gating tensions, upon dimerization of MscL. A combination of quantitative experiments on the spatial arrangement [24, 25] and gating tension [44, 54–57] of MscL would be able to put these predictions to a direct experimental test. The approach developed here represents a first step towards a physical theory of how elastic interactions affect the molecular structure, organization, and biological function of proteins in the crowded membrane environment provided by living cells.

[1] D. M. Engelman, Nature **438**, 578 (2005).
[2] T. Lang and S. O. Rizzoli, Physiology **25**, 116 (2010).
[3] J. U. Bowie, Nature **438**, 581 (2005).
[4] M. Milescu *et al.*, Nat. Struct. Biol. **16**, 1080 (2009).
[5] F. Bosmans, M. Milescu, and K. J. Swartz, Proc. Natl. Acad. Sci. U.S.A. **108**, 20213 (2011).
[6] S. G. Brohawn, J. del Mármol, and R. MacKinnon, Science **335**, 436 (2012).
[7] D. Schmidt, J. del Mármol, and R. MacKinnon, Proc. Natl. Acad. Sci. U.S.A., **109**, 10352 (2012).
[8] O. G. Mouritsen and M. Bloom, Annu. Rev. Biophys. Biomol. Struct. **22**, 145 (1993).
[9] K. Mitra, I. Ubarretxena-Belandia, T. Taguchi, G. Warren, and D. M. Engelman, Proc. Natl. Acad. Sci. U.S.A. **101**, 4083 (2004).
[10] D. Krepkiy *et al.*, Nature **462**, 473 (2009).
[11] Y. Sonntag *et al.*, Nat. Comm. **2**, 304 (2011).
[12] H. W. Huang, Biophys. J. **50**, 1061 (1986).
[13] M. Ø. Jensen and O. G. Mouritsen, Biochim. Biophys. Acta **1666**, 205 (2004).
[14] J. A. Lundbæk, J. Phys.: Condens. Matt. **18**, S1305 (2006).

[15] O. S. Andersen and R. E. Koeppe, II, Annu. Rev. Biophys. Biomol. Struct. **36**, 107 (2007).

[16] R. Phillips, T. Ursell, P. Wiggins, and P. Sens, Nature **459**, 379 (2009).

[17] J. A. Lundbæk, R. E. Koeppe, II, and O. S. Andersen, Proc. Natl. Acad. Sci. U.S.A. **107**, 15427 (2010).

[18] P. Greisen, Jr., *et al.*, Proc. Natl. Acad. Sci. U.S.A. **108**, 12717 (2011).

[19] T. A. Harroun, W. T. Heller, T. M. Weiss, L. Yang, and H. W. Huang, Biophys. J. **76**, 937 (1999).

[20] R. L. Goforth *et al.*, J. Gen. Physiol. **121**, 477 (2003).

[21] M. L. Molina *et al.*, J. Biol. Chem. **281**, 18837 (2006).

[22] A. V. Botelho *et al.*, Biophys. J. **91**, 4464 (2006).

[23] D. Baddeley *et al.*, Proc. Natl. Acad. Sci. U.S.A. **106**, 22275 (2009).

[24] S. L. Grage *et al.*, Biophys. J. **100**, 1252 (2011).

[25] T. Nomura *et al.*, Proc. Natl. Acad. Sci. U.S.A. **109**, 8770 (2012).

[26] N. Dan, P. Pincus, and S. A. Safran, Langmuir **9**, 2768 (1993).

[27] M. Goulian, R. Bruinsma, and P. Pincus, Europhys. Lett. **22**, 145 (1993).

[28] R. Golestanian, M. Goulian, and M. Kardar, Europhys. Lett. **33**, 241 (1996).

[29] R. Golestanian, M. Goulian, and M. Kardar, Phys. Rev. E **54**, 6725 (1996).

[30] H. Aranda-Espinoza, A. Berman, N. Dan, P. Pincus, and S. A. Safran, Biophys. J. **71**, 648 (1996).

[31] T. R. Weikl, M. M. Kozlov, and W. Helfrich, Phys. Rev. E **57**, 6988 (1998).

[32] K. S. Kim, J. Neu, and G. Oster, Biophys. J. **75**, 2274 (1998).

[33] K. S. Kim, J. C. Neu, and G. F. Oster, Europhys. Lett. **48**, 99 (1999).

[34] K. S. Kim, J. Neu, and G. Oster. Phys. Rev. E **61**, 4281 (2000).

[35] T. Chou, K. S. Kim, and G. Oster. Biophys. J. **80**, 1075 (2001).

[36] K. S. Kim, T. Chou, and J. Rudnick, Phys. Rev. E **78**, 011401 (2008).

[37] H.-K. Lin, R. Zandi, U. Mohideen, and L. P. Pryadko, Phys. Rev. Lett. **107**, 228104 (2011).

[38] A. D. Dupuy and D. M. Engelman, Proc. Natl. Acad. Sci. U.S.A. **105**, 2848 (2008).

[39] S. Takamori *et al.*, Cell **127**, 831 (2006).

[40] M. Lindén, P. Sens, and R. Phillips, PLoS Comput. Biol. **8**, e1002431 (2012).

[41] R. H. Spencer and D. C. Rees. Ann. Rev. Biophys. Biomol. Struct. **31**, 207 (2002).

[42] S. W. White, Nature **459**, 344 (2009).

[43] O. P. Hamill and B. Martinac, Physiol. Rev. **81**, 685 (2001).

[44] V. S. Markin and F. Sachs, Phys. Biol. **1**, 110 (2004).

[45] E. Perozo, Nat. Rev. Mol. Cell Biol. **7**, 109 (2006).

[46] I. R. Booth *et al.*, Nat. Rev. Microbiol. **5**, 431 (2007).

[47] E. S. Haswell, R. Phillips, and D. C. Rees, Structure **19**, 1356 (2011).

[48] M. R. Dorwart, R. Wray, C. A. Brautigam, Y. Jiang, and P. Blount, PLoS Biol. **8**, e1000555 (2010).

[49] C. S. Gandhi, T. A. Walton, and D. C. Rees, Prot. Sci. **20**, 313 (2011).

[50] I. Iscla, R. Wray, and P. Blount, Prot. Sci. **20**, 1638 (2011).

[51] G. Chang, R. H. Spencer, A. T. Lee, M. T. Barclay, and D. C. Rees, Science **282**, 2220 (1998).

[52] S. Sukharev, M. Betanzos, C.-S. Chiang, and H. R. Guy, Nature **414**, 720 (2001).

[53] S. Sukharev, S. R. Durrell, and H. R. Guy, Biophys. J. **81**, 917 (2001).

[54] E. Perozo, A. Kloda, D. M. Cortes, and B. Martinac, Nat. Struct. Biol. **9**, 696 (2002).

[55] E. Perozo, D. M. Cortes, P. Sompornpisut, A. Kloda, and B. Martinac, Nature **418**, 942 (2002).

[56] C.-S. Chiang, A. Anishkin, and S. Sukharev, Biophys. J. **86**, 2846 (2004).

[57] A. Anishkin, C.-S. Chiang, and S. Sukharev, J. Gen. Physiol. **125**, 155 (2005).

[58] U. Seifert, Adv. Phys. **46**, 13 (1997).

[59] D. Boal, *Mechanics of the Cell* (Cambridge University Press, Cambridge, 2002).

[60] S. A. Safran, *Statistical Thermodynamics of Surfaces, Interfaces, and Membranes* (Westview Press, Boulder, 2003).

[61] J.-B. Fournier, Eur. Phys. J. B **11**, 261 (1999).

[62] P. Wiggins and R. Phillips, Proc. Natl. Acad. Sci. U.S.A. **101**, 4071 (2004).

[63] P. Wiggins and R. Phillips, Biophys. J. **88**, 880 (2005).

[64] T. Ursell, K. C. Huang, E. Peterson, and R. Phillips, PLoS Comput. Biol. **3**, e81 (2007).

[65] T. Ursell *et al.*, in *Mechanosensitivity in Cells and Tissues 1: Mechanosensitive Ion Channels* (edited by A. Kamkin and I. Kiseleva, Springer-Verlag, 2008).

[66] C. Nielsen, M. Goulian, and O. S. Andersen, Biophys. J. **74**, 1966 (1998).

[67] N. Dan and S. A. Safran, Biophys. J. **75**, 1410 (1998).

[68] E. Zauderer, *Partial Differential Equations of Applied Mathematics* (John Wiley & Sons, Inc., New York, 1983).

[69] Mathematica 8.0, Wolfram Research, Inc., Urbana-Champaign, IL.

[70] See supplemental material at http://link.aps.org/supplemental/— for further details.

[71] Z. Liu, C. S. Gandhi, and D. C. Rees, Nature **461**, 120 (2009).

[72] N. Saint *et al.*, J. Biol. Chem. **273**, 14667 (1998).